Enhanced electron-lattice coupling in $La_{1-x}Sr_xMnO_3$ near the metal-insulator phase boundary

Y. Moritomo
Joint Research Center for Atom Technology (JRCAT), Tsukuba 305, Japan
and Center for Integrated Research for Science and Engineering (CIRSE), Nagoya University, Nagoya 464-01, Japan

A. Asamitsu
Joint Research Center for Atom Technology (JRCAT), Tsukuba 305, Japan

Y. Tokura
Joint Research Center for Atom Technology (JRCAT), Tsukuba 305, Japan
and Department of Applied Physics, University of Tokyo, Tokyo 113, Japan
(Received 9 July 1996; revised manuscript received 18 February 1997)

Effects of hydrostatic pressure on the magnetic and transport properties have been investigated for melt-grown crystals of $La_{1-x}Sr_xMnO_3$ with a finely-controlled doping level x near the metal-insulator phase boundary. Application of pressure affects the critical temperatures for the orthorhombic-rhombohedral structural transition (T_s) as well as for the metal-insulator transition (T_{MI}) that has been interpreted in terms of an ordering of the Jahn-Teller polarons. Reflecting that the kinetic energy of the e_g carriers sensitively depends on the degree of the lattice distortion, T_s shows an abrupt decrease under pressure when it crosses the magnetic phase boundary. On the other hand, T_{MI} is significantly suppressed under pressure via enhanced e_g-electron hopping. These pressure effects are compared with those of an external magnetic field. [S0163-1829(97)03243-8]

I. INTRODUCTION

Discovery of high-temperature superconductivity in hole-doped copper-oxide compounds has aroused renewed and extended interest in the correlated dynamics of spins and charges in the barely metallic state near the Mott transition in $3d$-transition-metal oxide systems. During the study, electronic properties of hole-doped manganites with perovskite-type structure, $R_{1-x}A_xMnO_3$, where R and A are trivalent rare-earth and divalent alkaline-earth ions, have been revisited to unveil their large magnetoresistance (MR) phenomena near the Curie temperature T_c.[1–5] Recent extensive studies have revealed that the doped manganites show a variety of phenomena besides the large MR effect, such as magneto-structural phase transition,[6,7] magnetovolume effect,[8] charge-ordering transition,[9–14] magnetic-field-induced insulator-to-metal transition,[15–18] and pressure-induced insulator-to-metal transition.[12,19] These phenomena are ascribed not only to the strong coupling between the itinerant e_g electrons and local t_{2g} spins mediated by a strong on-site exchange interaction (Hund's rule coupling, J_H),[20,21] but to the other instabilities, such as the Jahn-Teller (JT) instability[22] inherent to the MnO_6 octahedra, charge- and/or orbital-ordering instability, antiferromagnetic spin-fluctuation,[23] and so on. In this paper, we have investigated effects of hydrostatic pressure on the magnetic and transport properties for crystals of $La_{1-x}Sr_xMnO_3$ ($0.15 \leqslant x \leqslant 0.18$) with a fine interval of doping level x near the metal-insulator phase boundary. With use of an external pressure, we can control the carrier itineracy without changing the doping level.[24–26] The results suggest that the electron-lattice coupling plays an important role in the insulator-metal phenomena even for $La_{1-x}Sr_xMnO_3$ with a relatively large bandwidth W of the e_g band.

Crystals of $La_{1-x}Sr_xMnO_3$ ($x \geqslant 0.17$) are known to be conducting ferromagnets mediated by the double-exchange (DE) interaction.[20,21] The nominal Mn^{3+} ion in the insulating $LaMnO_3$ has the electron configuration of $t_{2g}^3 e_g^1$. The t_{2g}^3 electrons can be viewed as a local spin ($S=\frac{3}{2}$), while the e_g state strongly hybridized with the O $2p$ states and has an itinerant character when an appropriate number of vacancies (holes) is introduced. A distinct feature of doped manganites is that there exists a strong on-site exchange interaction J_H between the itinerant e_g carriers and local t_{2g} spins. As a result, transfer integral t of an e_g carrier is significantly affected by spin alignment as

$$t = t_0 \cos(\Delta\theta/2), \tag{1}$$

where t_0 is the bare-transfer integral and $\Delta\theta$ is the relative angle of the neighboring t_{2g} spins.[20] With hole-doping beyond $x_c = 0.17$ (Ref. 5) by substitution of the La^{3+} ions with the Sr^{2+} ions, the system turns into ferromagnetic metal (FM). In addition, change in the average ionic radius r_A of the perovskite A site alters the lattice structure from orthorhombic ($Pbnm$, $Z=4$; O) to rhombohedral ($R3c$, $Z=2$; R).[5] Resultant increase of the Mn-O-Mn bond angle toward 180° enhances the itineracy of the e_g carriers, which is manifested by reduction of resistivity at the structural transition. Thus, the kinetic energy of the e_g carriers correlates not only with the spin arrangement but with the lattice distortion.

Overall magnetic and transport properties of $La_{1-x}Sr_xMnO_3$ with maximal W are well reproduced by a dynamical mean-field approximation of the DE model,[4,27] which takes account of only t_0 and J_H. The MR phenomena

are explained in terms of reduction of the spin scattering of the e_g carriers by the forcibly aligned t_{2g} spins ($\Delta\theta \rightarrow 0$). To explain the ''colossal'' value of the MR for the systems with smaller W, e.g., $La_{1-x}Sr_xCa_xMnO_3$ (Ref. 8) and $(Nd,Sm)_{1/2}Sr_{1/2}MnO_3$,[28] however, we need additional mechanisms for carrier localization above T_c. Millis, Littlewood, and Shraiman[22] have argued that effect of the JT interaction inherent to the MnO_6 octahedra is essential for understanding the transport properties of doped manganites, in particular a large resistivity value above T_c. This idea is supported by some neutron diffraction measurements,[29,30] which indicates release of the distortion of the MnO_6 octahedra in the FM phase. Another candidate may be the charge- and/or orbital-ordering instability, especially when x approaches a commensurate value. In several manganite compounds, e.g., $Nd_{1/2}Sr_{1/2}MnO_3$, the instability causes a charge-ordering transition,[9] that is, real-space ordering of the doped carriers. The charge-ordering transition is no more present for $La_{1-x}Sr_xMnO_3$ than with maximal W.[12] Recently, Yamada *et al.*[31] proposed that ordering of the JT polarons takes place around $x=\frac{1}{8}$ at low temperature on the basis of their neutron diffraction results.

The format of the present paper is as follows. In Sec. II, we describe crystal-growth procedure for $La_{1-x}Sr_xMnO_3$ as well as details of the high-pressure experiment. Electronic and structural phase diagrams are presented in Sec. III. A part of the results on the phase diagram and the effect of an external magnetic field on the transport properties has been published in separate papers.[5–7] Here, we describe details of pressure effects on the magnetic and transport properties near the metal-insulator phase boundary. In Sec. IV, we discuss effects of pressure on the structural transition. The critical temperature T_s shows an abrupt decrease when it crosses the magnetic phase boundary, suggesting a strong coupling between the spin arrangement and lattice distortion. In a previous paper,[6,7] we have reported the effect of an external magnetic field on this transition. We will compare the present pressure effect with the magnetic-field effect. Section V is devoted to pressure effects on the ferromagnetic but insulating (FI) state, which can be viewed as an ordered state of JT polarons. Application of pressure promotes the FI-to-FM transition and eventually, the FI state disappears. A summary is given in Sec. VI.

II. EXPERIMENT

Crystals of $La_{1-x}Sr_xMnO_3$ ($0.12 \leqslant x \leqslant 0.18$) were grown by the floating-zone method at a feeding speed of 5–10 mm/h.[5,24] A stoichiometric mixture of La_2O_3, $SrCO_3$, and Mn_3O_4 was ground and calcined three times at 1050 °C for 24 h with an intermittent grinding procedure. Then resulting powder was pressed into a rod with a size of 5 mm$\phi \times$60 mm and sintered at 1350 °C for 24 h. Over the whole concentration range, the ingredient could be melted congruently in a flow of air. To characterize the crystals, powder x-ray diffraction measurements as well as electron-probe microanalysis (EPMA) was carried out. The results indicated that the obtained crystals are single phase and show a nearly identical composition with the prescribed one. With increasing x, the room-temperature structure changes from orthorhombic to rhombohedral at a critical concentration of $x_s \approx 0.17$.

A hydrostatic pressure was obtained with clamp-type piston cylinder cells. The pressures quoted in the paper were those measured at room temperature (Figs. 4 and 7). For low-pressure experiments (Figs. 4 and 5), a pressure cell, whose sample room size is 6 mm in diameter, was used. We have calibrated the pressure cell with the use of a ferromagnetic transition temperature of KH_2PO_4 crystal,[32] and found that relaxation of the pressure is less than $-2\%/100$ K below ~ 1 GPa. The sample temperature was monitored with a copper-Constantan thermocouple placed in the sample room, and was slowly increased or decreased at a rate of ≈ 10 K/h near the structural transition. To lower the sample temperature down to ~ 4 K (Figs. 7 and 8), a smaller-size pressure cell, whose piston size is 4 mm in diameter, was used with an AuFe(0.07%)-Chromel thermocouple attached near the sample room. T_C of lead[33] was used for calibration of the cell; it is inferred that the applied pressure relaxes at a rate of $-7\%/100$ K. Resistivity ρ was measured with the four-probe method using heat-treatment-type silver paint as electrodes. A small piece of crystal ($\sim 0.5 \times 1 \times 2$ mm^3) was placed in the sample room, which was filled with silicone oil as a pressure-transmitting medium. We also measured ac susceptibility χ under pressures to determine T_C.[24] A small piece of crystal (~ 10 mg) was placed in a coil (2 mm in diameter and ≈ 10 mm in length) and inductance of the coil was monitored with a LCR meter at a frequency of 1 MHz. Pressure-induced changes in the ρ-T and χ-T curves were reproducible in repeated pressure cycles.

III. ELECTRONIC AND STRUCTURAL PHASE DIAGRAM

Before presenting details of experimental results, let us survey the x dependence of resistivity ρ for $La_{1-x}Sr_xMnO_3$. Figure 1 shows the ρ-T curves for $La_{1-x}Sr_xMnO_3$ with a fine interval of x ($0.12 \leqslant x \leqslant 0.18$). An arrow indicates T_C, which was determined from the χ-T curve. For $x \geqslant 0.14$, the ρ-T curve shows a jump (indicated by a triangle) due to the R-O structural transition.[6,7] The critical temperature T_s for the structural transition rapidly decreases with x from ≈ 430 K for $x=0.14$ to ≈ 150 K for $x=0.18$, and eventually disappears for $x=0.25$ (not shown). On the other hand, in the concentration range of $0.14 \leqslant x \leqslant 0.17$, the ρ-T curve shows a broad upturn in the ferromagnetic phase. We have confirmed that the magnetization curve (M-T) at 5 K is that of a prototypical ferromagnet, and steeply increases up to $\approx 4\,\mu_B$ above $\mu_0 H \approx 0.3$ T. Hereafter, we call the nonmetallic ($d\rho/dT < 0$) region the ferromagnetic insulator (FI) phase and define the critical temperature T_{MI} as the local minimum of the ρ-T curve. Recently, Yamada *et al.*[31] performed a neutron scattering experiment for $La_{0.85}Sr_{0.15}MnO_3$ ($x=0.15$) and have observed growth of superlattice reflections below $T_{\mathrm{MI}} \approx 200$ K. They have ascribed the reflections to regular ordering of the JT polarons. Beyond $x=0.18$, metallic conduction survives down to the lowest temperature. We summarize in Fig. 2 the x-T phase diagram for $La_{1-x}Sr_xMnO_3$. The eye-guiding solid and broken curves represent electronic and structural, phase boundaries, respectively.

One may notice another set of anomalies (filled triangles) in the ρ-T curves for $x=0.12$. These anomalies seem to be

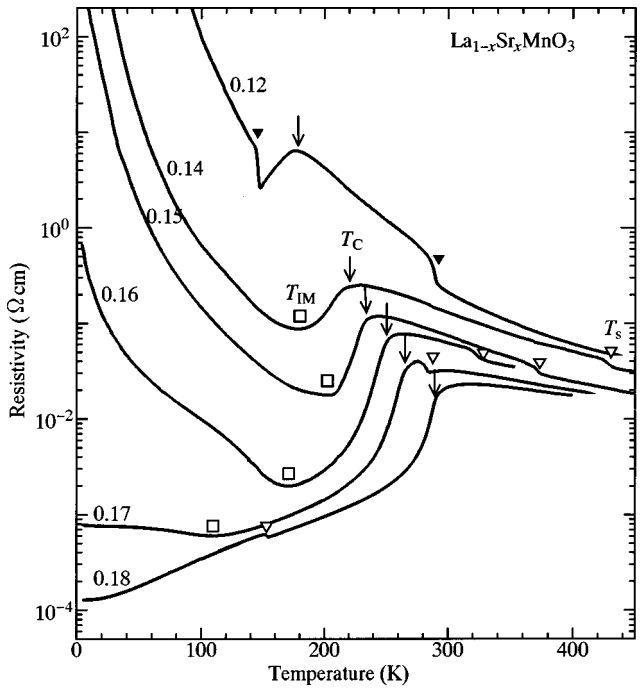

FIG. 1. Temperature dependence of resistivity for crystals of $La_{1-x}Sr_xMnO_3$ ($x=0.12-0.18$) in the warming run. T_c, T_s, and T_{MI} represent the Curie temperature, the critical temperature for the orthorhombic-rhombohedral structural transition, and that for the metal-insulator transition, respectively.

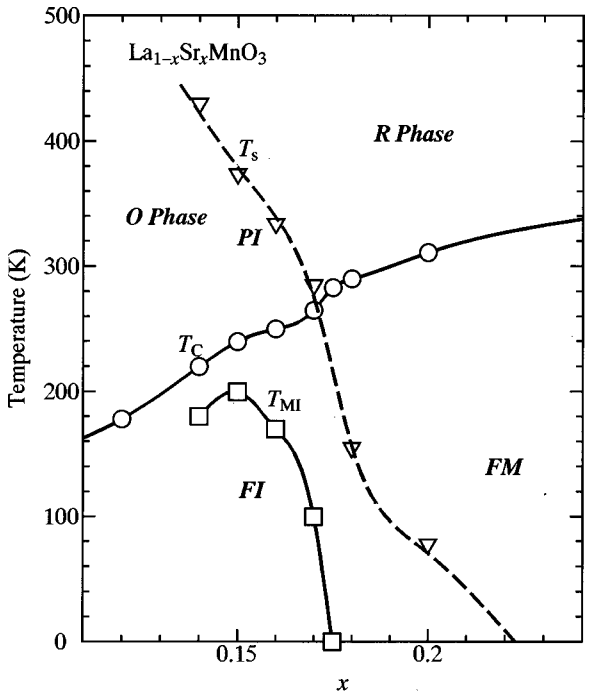

FIG. 2. Electronic and structural phase diagram for $La_{1-x}Sr_xMnO_3$. Circles and triangles stand for the Curie temperature T_c and the critical temperature T_s for the orthorhombic-rhombohedral structural transition, respectively (cited from Refs. 5 and 7). Squares stand for the critical temperature T_{MI} for the metal-insulator transition. A broken curve is the guide to the eye for the structural-phase boundary, while solid curves are for the electronic boundaries. PI, FI, and FM stand for paramagnetic insulator, ferromagnetic insulator, and ferromagnetic metal, respectively.

related to distortion of the MnO_6 octahedra as well as change in the spin structure. Argyriou *et al.*[30] have investigated temperature variation of the Mn-O bond length for $La_{0.185}Sr_{0.125}MnO_3$ ($x=0.125$) and found an anomalous distortion of the MnO_6 octahedra in the temperature range of 150–280 K, which the two filled triangles in Fig. 1 bracket. On the other hand, Kawano *et al.*[34] have observed a magnetic transition into a canted antiferromagnetic state below $T_{CA}\approx 150$ K for $x=0.125$, which coincides with the lower-lying anomaly observed in the ρ-T curve for $x=0.12$ crystal.

IV. EFFECT OF PRESSURE ON THE STRUCTURAL TRANSITION

In the doped manganites, applications of pressure enhances carrier itineracy, and hence strengthens the DE interaction.[19,24] Such a pressure-enhanced carrier itineracy is expected to also affect the structural transition near the metal-insulator phase boundary. First, let us scrutinize the χ-T and ρ-T curves for $x=0.17$ at ambient pressure (Fig. 3). With decreasing temperature, the χ value steeply rises at $T_C(=265$ K) accompanying a decrease of the ρ value. Value of T_C can be determined precisely from the inflection point of the χ-T curve with an error of ± 0.3 K. In the paramagnetic phase, a distinct hysteretic change is observed in the ρ-T curve around ≈ 283 K. This anomaly is originated in the O-R structural transition, because the orthorhombic (022) peak in the powder x-ray diffraction pattern for $x=0.17$ disappears above ≈ 285 K.[7] Thus, we can use the inflection point in the χ-T curve and the resistivity jump as sensitive monitors for T_C and T_s, respectively.

Figure 4 shows pressure dependence of (a) ac susceptibility and (b) resistivity for the $x=0.17$ crystal. Reflecting the pressure-enhanced carrier itineracy, T_C increases from 265 K at ambient pressure to 282 K under pressure of 0.32 GPa. By contrast, T_s decreases from ≈ 280 K ($\geqslant T_C$) at ambient pressure to ≈ 230 K ($\leqslant T_C$) at 0.24 GPa. In the intermediate pressure region, the structural transition takes places below T_C in the cooling run, but above T_C in the warming run. Accordingly, the χ-T curve shows an apparent hysteretic behavior [see, for example, the 0.12 GPa run in Fig. 4(a)] due to different Curie temperatures in both the O and R phases.

Thus obtained T_C and T_s are plotted in Fig. 5 against calibrated pressure. T_C and T_s are nearly pressure independent below 0.1 GPa. With further increase of pressure, T_s drops by ≈ 50 K from ≈ 250 to ≈ 230 K accompanying a jump of T_C by ≈ 10 K. Such a strong coupling between the lattice and spin system is perhaps mediated by the kinetic energy of the e_g carriers. In the doped manganites, transfer integral t of e_g carriers significantly increases in the spin-polarized FM phase ($t\rightarrow t_0$). Then, the energy gain in metallic state stabilizes the R structure with larger t_0 even at the cost of the elastic energy, which causes the discontinuous drop of T_s as observed. This argument is consistent with much smaller pressure effect for $x=0.175$ (see inset of Fig. 5), in which T_s locates in the FM phase ($T_s<T_C$).

The suppression of T_s under pressures is quite analogous to that induced by an external magnetic field H. Asamitsu *et al.*[6,7] have investigated effects of magnetic field on T_s, and derived the structural phase diagram in the H-T plane:

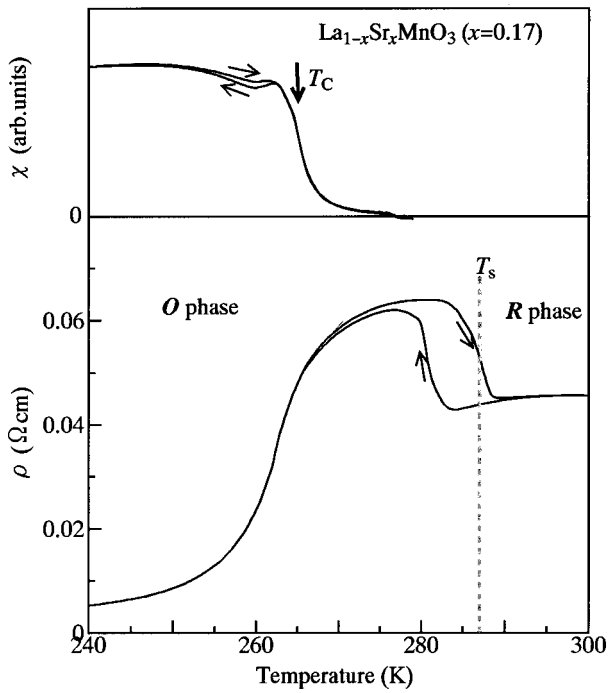

FIG. 3. Temperature-variation of ac susceptibility (upper panel) and resistivity (lower panel) for a crystal of $La_{0.83}Sr_{0.17}MnO_3$ ($x=0.17$). T_c and T_s represent the Curie temperature and the critical temperature for the orthorhombic-rhombohedral structural transition, respectively.

T_s discontinuously decreases by ≈ 40 K from ≈ 280 to ≈ 240 K at a field of ≈ 2 T. The magnetic field aligns the local t_{2g} spins [$\Delta\theta \rightarrow 0$ in Eq. (1)], and hence increases the carrier itineracy. Thus, the application of an external magnetic field has qualitatively the same effect as the pressure application, and hence stabilizes the R phase as observed. However, effects of the magnetic field on the transport properties are restricted near T_C and become negligible far below T_C.[6,7] This makes a sharp contrast with the pressure effect that induces a nearly uniform reduction of resistivity independent of temperature [see Fig. 4(b)].

V. EFFECT OF PRESSURE ON THE METAL-INSULATOR TRANSITION

Near the metal-insulator phase boundary, a ferromagnetic but insulating (FI) phase appears (see Fig. 2). As a prototypical example, we show in Fig. 6 temperature variation of ρ and M for $x=0.16$ at ambient pressure. With decreasing temperature, the ρ value gradually increases below $T_{\mathrm{MI}} \approx 170$ K accompanying a small anomaly in the M-T curve. It is plausible that the JT polarons are thermally activated and barely mobile in the temperature range of $T_{\mathrm{MI}} \leq T \leq T_C$, but are weakly localized when forming a polaron lattice at lower temperature ($\leq T_{\mathrm{MI}}$). The weakly localized e_g carriers can mediate the DE interaction between the neighboring t_{2g} spins and cause the ferromagnetic state. Recently, Yamada *et al.*[31] have proposed that such a polaron lattice is induced below T_{MI} on the basis of their neutron diffraction results. Nominal hole concentration corresponding to the proposed polaron lattice periodicity is $x=\frac{1}{8}$.

The external pressure has significant effects on the MI

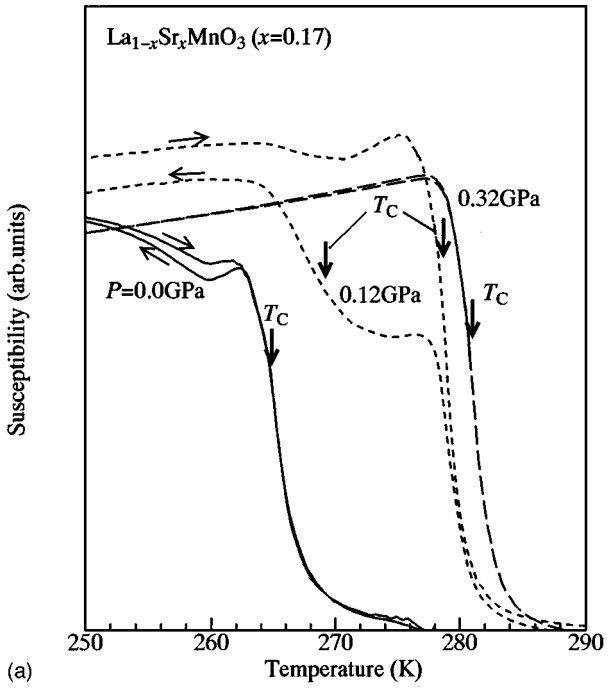

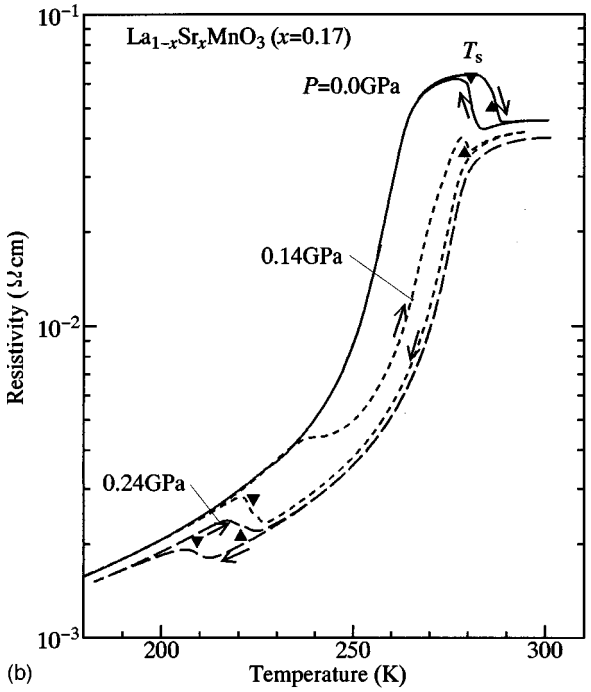

FIG. 4. Pressure dependence of (a) ac susceptibility and (b) resistivity for a crystal of $La_{0.83}Sr_{0.17}MnO_3$ ($x=0.17$). Filled triangles and arrows represent T_s and T_c, respectively.

transition. In Fig. 7 are shown the ρ-T curves under pressures. With increase of pressure, enhanced carrier itineracy (or polaron hopping) converts the FI phase to the FM phase and eventually the FI phase disappears above ~ 0.14 GPa. Incidentally, an abrupt change of T_C between $P=0.4$ and 0.7 GPa is due to the intersection of the magnetic phase boundary and the structural one. In Fig. 8, we plot T_{MI} against calibrated pressure: a solid curve is for $x=0.16$ and a broken curve for $x=0.15$. With an increase in pressure, the MI phase boundary shifts toward the low-temperature side in a

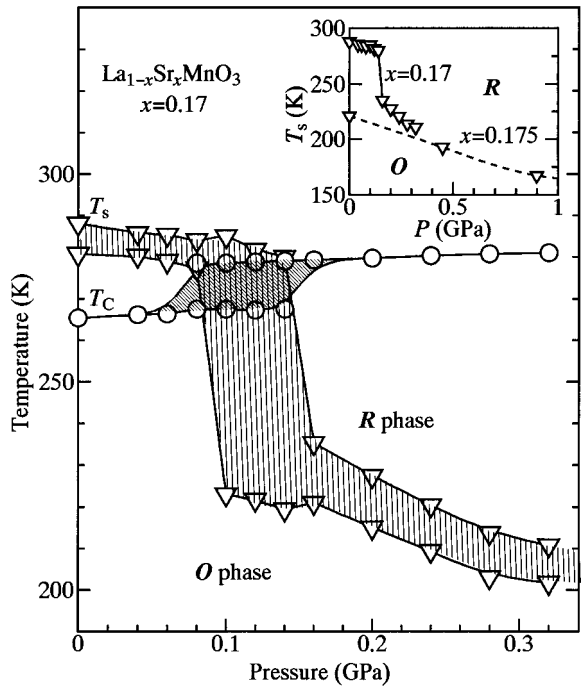

FIG. 5. Pressure-temperature phase diagram for $La_{0.83}Sr_{0.17}MnO_3$ ($x=0.17$). Triangles and circles represent T_s and T_c, respectively. The hatching regions represent the thermal hysteresis. Inset shows comparison of the structural phase boundaries (in the warming run) for $x=0.17$ and 0.175. Note that the horizontal axis is the calibrated pressure.

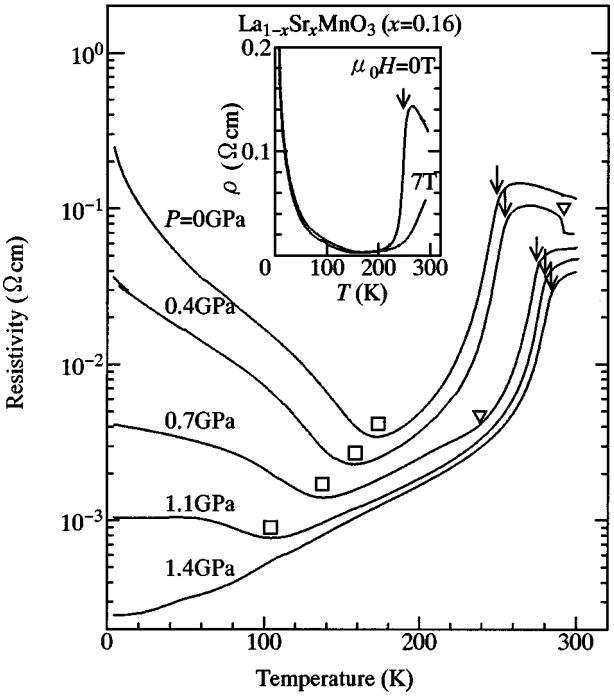

FIG. 7. Pressure dependence of resistivity for a crystal of $La_{0.84}Sr_{0.16}MnO_3$ ($x=0.16$). Squares, triangles, and arrows represent T_{MI}, T_s, and T_c, respectively. Inset shows effect of an external magnetic field on the resistivity.

strongly x-dependent manner. The FI state completely disappears above ≈ 0.11 GPa for $x=0.16$, while the phase remains even at ≈ 1.6 GPa for $x=0.15$. Robustness of the FI phase for $x=0.15$ is perhaps ascribed to proximity of x to the commensurate value ($x=\frac{1}{8}$) as well as to the reduced total kinetic energy of the carriers.

It should be noted that an external magnetic field has a negligible effect on this MI transition. As seen in the inset of Fig. 7, a magnetic field scarcely affects the transport properties below 200 K apart from the conventional MR effect around T_c. This is because the MI transition takes place in

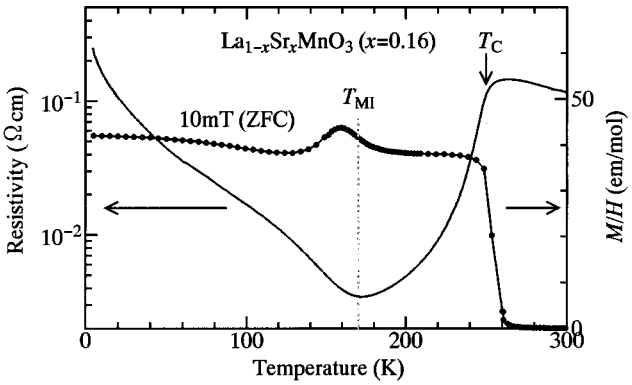

FIG. 6. Temperature-variation of resistivity and magnetization (measured under a field of 10 mT) for a crystal of $La_{0.84}Sr_{0.16}MnO_3$ ($x=0.16$). Magnetization was measured after cooling down to 5 K in zero field (ZFC). T_C and T_{MI} represent the Curie temperature and the critical temperature for the metal-insulator transition, respectively.

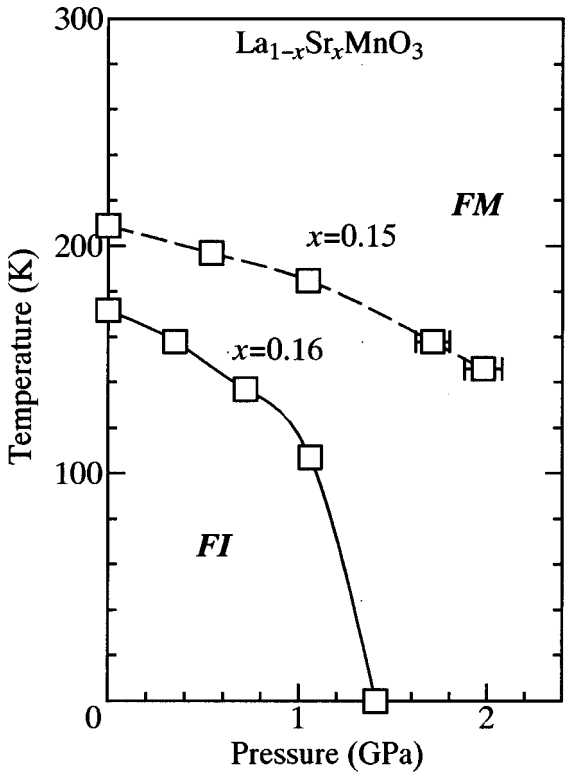

FIG. 8. Pressure dependence of T_{MI} for $x=0.16$ and 0.17. Note that the horizontal axis is the calibrated pressure. FI and FM represent ferromagnetic insulator and ferromagnetic metal, respectively.

the FM phase with sufficient spin polarization, and hence the coupling between the conduction electrons and local spins plays a minor role. This makes a sharp contrast with the case of the structural transition at T_s (see Sec. IV) as well as the resistive change around T_C.[24]

VI. SUMMARY

We have investigated the effects of pressure on the magnetic and transport properties for $La_{1-x}Sr_xMnO_3$ with a fine interval of x near the metal-insulator phase boundary. Application of pressure significantly affects (1) the orthorombic-rhombohedral structural transition at T_s and (2) the metal-insulator transition at T_{MI} that has been interpreted in terms of the ordering of the JT polarons. Reflecting the strong correlation of the kinetic energy of the e_g carriers with the lattice distortion, T_s shows an abrupt reduction under pressure when it crosses the magnetic phase boundary. An external magnetic field also increases the carrier itineracy, and hence has similar effect on T_s. On the other hand, an application of pressure destabilizes the ordered state of the JT polarons below T_{MI} via enhanced e_g-electron hopping. In this case, however, magnetic field has negligible effect on T_{MI}, suggesting that the electron-spin interaction plays a minor role on this transition. These observations indicate that electron-lattice coupling plays significant roles in the transport properties even for $La_{1-x}Sr_xMnO_3$ with maximal bandwidth near the metal-insulator phase boundary.

ACKNOWLEDGMENTS

This work was supported by the New Energy and Industrial Technology Development Organization (NEDO) of Japan and by a Grant-In-Aid for Scientific Research from the Ministry of Education, Science, and Culture, Japan. The authors are grateful to K. Hirota, H. Kawano, H. Yoshizawa, T. Inami, and Y. Yamada for fruitful discussions, and also to T. Kimura for his help in calibration of the pressure cells.

[1] K. Chahara, T. Ohno, M. Kasai, and Y. Kozono, Appl. Phys. Lett. **63**, 1990 (1993).
[2] R. von Helmont, J. Wecker, B. Holzapfel, M. Schultz, and K. Samwer, Phys. Rev. Lett. **71**, 2331 (1993).
[3] S. Jin, T.H. Tiefel, M. McCormack, R. Fastnacht, R. Ramesh, and L. H. Chen, Science **264**, 13 (1994).
[4] Y. Tokura, A. Urushibara, Y. Moritomo, T. Arima, A. Asamitsu, and G. Kido, J. Phys. Soc. Jpn. B **63**, 3931 (1994).
[5] A. Urushibara, Y. Moritomo, T. Arima, A. Asamitsu, G. Kido, and Y. Tokura, Phys. Rev. B **51**, 14 103 (1995).
[6] A. Asamitsu, Y. Moritomo, Y. Tomioka, T. Arima, and Y. Tokura, Nature (London) **373**, 407 (1995).
[7] A. Asamistu, Y. Moritomo, R. Kumai, Y. Tomioka, and Y. Tokura, Phys. Rev. B **54**, 1716 (1996).
[8] M. R. Ibarra, P. A. Algarabel, C. Marquina, J. Blasco, and J. Garcia, Phys. Rev. Lett. **75**, 3541 (1995).
[9] H. Kuwahara, Y. Tomioka, A. Asamitsu, Y. Moritomo, and Y. Tokura, Science **270**, 961 (1995).
[10] Y. Tomioka, A. Asamitsu, Y. Moritomo, H. Kuwahara, and Y. Tokura, Phys. Rev. Lett. **74**, 5108 (1995).
[11] Y. Tokura, H. Kuwahara, Y. Moritomo, Y. Tomioka, and A. Asamitsu, Phys. Rev. Lett. **76**, 3184 (1996).
[12] Y. Moritomo, H. Kuwahara, Y. Tomioka, and Y. Tokura, Phys. Rev. B **55**, 7549 (1997).
[13] A. P. Ramirez, P. Schiffer, S-W. Cheong, C. H. Chen, W. Bao, T. T. M. Palstra, P. L. Gammel, D. J. Bishop, and B. Zegarski, Phys. Rev. Lett. **76**, 3188 (1996).
[14] Y. Moritomo, Y. Tomioka, A. Asamitsu, and Y. Tokura, Phys. Rev. B **51**, 3297 (1995); B. J. Sternlieb, J. P. Hill, U. C. Wildgruber, G. M. Luke, B. Nachumi, Y. Moritomo, and Y. Tokura, Phys. Rev. Lett. **76**, 2169 (1996).
[15] Y. Tomioka, A. Asamitsu, Y. Moritomo, and Y. Tokura, J. Appl. Phys. **64**, 3264 (1995).
[16] Y. Tomioka, A. Asamitsu, H. Kuwahara, Y. Moritomo, and Y. Tokura, Phys. Rev. B **53**, 1689 (1996).
[17] H. Y. Hwang, S-W. Cheong, P. G. Radaeli, M. Marezio, and B. Batlogg, Phys. Rev. Lett. **75**, 914 (1995).
[18] M. R. Lees, J. Barratt, G. Balakrishana, D. McK. Paul, and M. Yethiray, Phys. Rev. B **52**, 14 303 (1995).
[19] H. Y. Hwang, T. T. M. Palstra, S-W. Cheong, and B. Batlogg, Phys. Rev. B **52**, 15 046 (1995).
[20] P. W. Anderson and H. Hasagawa, Phys. Rev. **100**, 675 (1955).
[21] P-G. de Gennes, Phys. Rev. **118**, 141 (1960).
[22] A. J. Millis, P. B. Littlewood, and B. I. Shraiman, Phys. Rev. Lett. **74**, 5144 (1994); **77**, 175 (1996).
[23] M. Kataoka, Czech. J. Phys. **46**, 1857 (1996).
[24] Y. Moritomo, A. Asamitsu, and Y. Tokura, Phys. Rev. B **51**, 16 491 (1995).
[25] X. Obradors, L. M. Paulius, M. B. Maple, J. B. Torrance, A. I. Nazzal, I. Fontcuberta, and X. Granados, Phys. Rev. B **47**, 12 353 (1993); P. L. Canfield, J. D. Thompson, S-W. Cheong, and L. W. Rupp, *ibid.* **47**, 12 357 (1993).
[26] Y. Okada, T. Arima, Y. Tokura, C. Maruyama, and N. Mori, Phys. Rev. B **48**, 9677 (1993).
[27] N. Furukawa, J. Phys. Soc. Jpn. **63**, 3214 (1994); **64**, 2734 (1995); **64**, 2754 (1995); **64**, 3164 (1995).
[28] H. Kuwahara, Y. Tomioka, Y. Moritomo, A. Asamitsu, M. Kasai, R. Kumai, and Y. Tokura, Science **272**, 80 (1996).
[29] P. G. Radaelli, D. E. Cox, M. Marezio, S-W. Cheong, P. E. Schiffer, and A. P. Ramirez, Phys. Rev. Lett. **75**, 4488 (1995).
[30] D. N. Argyriou, J. F. Mitchell, C. D. Potter, D. G. Hinks, J. D. Jorgensen, and S. D. Bader, Phys. Rev. Lett. **76**, 3826 (1996).
[31] Y. Yamada, O. Hino, S. Nohdo, R. Kanao, T. Inami, and S. Katano, Phys. Rev. Lett. **77**, 904 (1996).
[32] G. A. Samara, Phys. Rev. Lett. **27**, 103 (1971).
[33] T. F. Smith and C. W. Chu, Phys. Rev. **159**, 353 (1967).
[34] H. Kawano, R. Kajimoto, M. Kubota, and H. Yoshizawa, Phys. Rev. B **53**, 2202 (1996).